Journal of Scientific Computing (2019) 79:517–541
https://doi.org/10.1007/s10915-018-0858-8

A Local Radial Basis Function Method for Pricing Options Under the Regime Switching Model

Hengguang Li[1] · Reza Mollapourasl[2,3] · Majid Haghi[2]

Received: 12 May 2017 / Revised: 10 July 2018 / Accepted: 13 October 2018 /
Published online: 26 October 2018

Abstract
This paper is devoted to develop an efficient meshfree method based on radial basis functions (RBFs) to solve a system of partial differential equations arising from pricing options under the regime switching model. For global RBF methods, one of the major disadvantages is the computational cost and ill-conditioning associated with the dense linear systems that arise. So, we employ one of the local meshfree methods known as radial basis function based finite difference method. Then with an operator splitting method, sparse and well-conditioned system of complementarity problems are solved very fast for the American option. Also, the uniqueness of solution is proved for the discretized system of equations. Numerical examples presented in the last section illustrate the robustness and practical performance of the proposed algorithm for pricing European and American options.

Keywords Radial basis functions · Finite difference · Option pricing · Regime switching model

1 Introduction

It is well known that a financial model which follows a stochastic process having constant volatility is not consistent with market prices. Recent studies have shown that models based on stochastic volatility, jump diffusion, and regime switching processes produce better fits to the market data. Unlike the standard Black–Scholes model [8] which assumes that the underlying assets follow a geometric Brownian motion with constant mean return and volatility, the rationale behind the regime switching framework is that the market may switch from time

✉ Reza Mollapourasl
mollapour@srttu.edu

Hengguang Li
li@wayne.edu

Majid Haghi
majidhaghi@sru.ac.ir

1 Department of Mathematics, Wayne State University, Detroit, MI 48202, USA

2 School of Mathematics, Shahid Rajaee Teacher Training University, 16788, Lavizan, Tehran, Iran

3 Department of Mathematics, Oregon State University, Corvallis, OR 97331, USA

to time among different regimes. In short-term political or economic uncertainty, this property of regime switching model help us to account for certain periodic or cyclic patterns. In many practical researches such as [4] regime switching model has been used widely. Recent empirical research suggests that regime switching model describe the time series properties of several important financial variables, including interest rates and exchange rates, more accurately than single-regime alternatives. Some of regime switching applications are insurance [23], electricity markets [22,44], natural gas [1,13], optimal forestry management [12], trading strategies [14], valuation of stock loans [51], and interest rate dynamics [29].

In this work, we present a numerical method to evaluate European and American options under the regime switching model. The prices of European and American options under the regime switching are derived by solving a system of PDEs. A variety of numerical methods are proposed to price an European or American option when the underlying asset follows a regime switching model. In [5] a global RBF collocation method for pricing the American options is presented. For pricing American options under a regime switching stochastic process, in [26] both explicit and implicit discretizations with the focus on methods which are unconditionally stable are investigated, and they conclude, their technique which is implemented for the American problem as an abstract optimal control problem; hence they can use their results to more general problems as well. In [33], author used a tree method for pricing European and American options under the regime switching model, and under some conditions positivity of branch probabilities is granted. Also, this method is considered in [34] for pricing both European and American options in a regime switching jump diffusion model with state-dependent regime switching rates.

In [30], authors present a combination of the penalty method for dealing with linear complimentary problem (LCP) and an exponential time differencing Crank–Nicolson method employed for time discretization for numerical solution of the American option pricing problem in the regime switching model. The numerical method based on multivariable front-fixing transformation is employed in [16] for solving a system of PDE with a free boundary arising in the American option pricing problem under the regime switching model. In [31], a numerical scheme via a combination of an implicit implementation of the θ-method and a penalty scheme for solving a regime switching American option pricing model is developed. Also, in [50] a second-order method based on exponential time differencing approach is proposed for solving American options under multi-state regime switching. For dealing with free boundary problems, they use a penalty method, and stability and convergence of the method are considered.

Iterated optimal stopping method has been used as the basis of a numerical algorithm for American options under the regime switching in [32]. Then local policy iteration method as an alternative method has been suggested in [26,40]. Also, comparison of these two methods has been done for American options under the regime switching model in [2]. In [47] a combination of finite element method with Crank–Nicolson time discretization technique and a simple lattice method are proposed for numerical valuation of American options under a regime switching model. Also, stability analysis of the method is discussed. Some conjectures about the position of early exercise prices were presented in [47], and then in [24] those conjectures are proved.

Meshfree methods based on RBFs are of general interest for solving PDEs, because they can provide high-order or spectral convergence for smooth solutions in complex geometries. In [3,17], meshfree methods based on RBF approximation have been shown to perform better than finite difference methods for option pricing problems in one and two spatial dimensions. Similar problems have also been solved in [25,46]. Also, in [38], a meshfree radial basis point interpolation method is used for solving the Black–Scholes model for European and

American options which has some advantages in compare with the conventional meshfree methods. Global radial basis function method is employed in [36] for pricing of financial contracts, and also authors have shown that the proposed scheme is second order accurate in time and spectrally accurate in space for constant shape parameter.

However, all of these papers employ global RBF collocation methods, leading to dense linear systems, and computational costs that become prohibitive as the number of dimensions increase. Localized RBF approximations such as the RBF partition of unity collocation method (RBF-PUM) and RBF-FD give an answer to deal with these issues. In [20] local meshless approach based on radial basis functions generated by finite difference is presented to price the options under the Black–Scholes model. Also, they derived that the proposed method is unconditionally stable. In [35], we price American options under Heston's stochastic volatility model using RBF-PUM applied to a linear complementary formulation of the free boundary partial differential equation problem.

In the present paper, we use RBF-FD method in spatial discretization of a system of partial differential equations arisen from European and American option pricing problem under the regime switching model. Although RBF-FD method has been implemented in various favors and contexts in the last 10 years, the first survey articles on RBF-FD are just emerging in [18,19]. The matrices formed during the localized RBF-FD method will be sparse and, hence, will not suffer from ill-conditioning and high computational costs. For temporal discretization, we apply the implicit method with two time levels. In American options, we solve an sparse and well-conditioned disceretized LCP instead of free boundary problem by using an operator splitting method defined in [28].

In the next section, we describe the regime switching model and a system of partial differential equations for pricing European option, then we formulate the American option pricing problem as an LCP. RBF-FD approximation is introduced in Sect. 3, then applied for spatial discretizarion in Sect. 4. Time discretizarion for semidiscrete system of equations arisen in European option as well as LCP derived from American option pricing problem are presented in Sect. 5. Then, we prove that the full discrete system of equations has a unique and stable solution in Sect. 6. Finally, in the last section, the accuracy and efficiency of the proposed method is numerically investigated for European and American options, and compared with existing methods in the literature.

2 Regime Switching Model

Suppose $(\Omega, \mathscr{F}, \mathscr{P})$ is a complete probability space, where $\mathscr{P}$ is a reference physical probability measure. Let $\mathscr{T}$ denote the time index set $[0, T]$ of the model. We suppose that the underlying asset switches among a finite number of states $\mathscr{M} := \{1, 2, \ldots, m\}$, which is modeled by a finite Markov chain $X(t)$. Also, we can identify the state space of $X(t)$ with a finite set of unit vectors $\{\mathbf{e}_1, \mathbf{e}_2, ..., \mathbf{e}_m\}$, where $\mathbf{e}_i = (0, ..., 1, ..., 0) \in \mathbb{R}^m$. Then the stock price process $S(t)$ is assumed to follow the stochastic differential equation

$$\frac{dS(t)}{S(t)} = r_{X(t)}dt + \sigma_{X(t)}dW(t), \quad t \in \mathscr{T}$$

where $r_{X(t)}$ is the risk-free interest rate, $\sigma_{X(t)}$ is the volatility of the asset $S(t)$, and $W(t)$ is a standard Brownian motion, also $r_{\mathbf{e}_i}$ and $\sigma_{\mathbf{e}_i}$ are constant when the economy is in the ith state

at time t, that is, $X(t) = \mathbf{e}_i$. Then we have the regime generator of $X(t)$ by an $m \times m$ matrix

$$\mathbf{Q} = \begin{pmatrix} q_{11} & \cdots & q_{1m} \\ \cdots & \cdots & \cdots \\ q_{m1} & \cdots & q_{mm} \end{pmatrix}.$$

From Markov chain theory [48], the entries of generator matrix satisfy

1. $q_{ij} \geq 0$ if $i \neq j$.
2. $\sum_{j=1}^{m} q_{ij} = 0$ for each $i \in \mathscr{M}$.

Now, we let $V_i(S(t), t)$ denote the time t price of an European option with asset price S_t at regime $X(t) = \mathbf{e}_i$. Under the equivalent martingale measure $\mathbb{Q}$, the risk-neutral value of this option with exercise price S_0 and time to maturity T is defined as its expected discounted payoff given by

$$V_i(S(t), t) = \mathbb{E}^{\mathbb{Q}}\left[e^{-r_{X(t)}(T-t)} P^{(X(t))}(S(T)) | X(t) = \mathbf{e}_i\right],$$

where under each regime, the payoff for call option is defined by $P^{(X(t))}(S(T)) = \max(S(T) - S_0, 0)$ and for put option is defined by $P^{(X(t))}(S(T)) = \max(S_0 - S(T), 0)$.

As in [11], using Itô's differentiation rule and the fact that $V_i(S, t)$ is a $\mathbb{Q}$ martingale, $V_i(S, t)$ satisfies the following regime switching partial differential equation

$$\frac{\partial V_i(S,t)}{\partial t} + \frac{1}{2} S^2 \sigma_i^2 \frac{\partial^2 V_i(S,t)}{\partial S^2} + r_i S \frac{\partial V_i(S,t)}{\partial S} - r_i V_i(S,t) + < \mathbf{QV}(S,t), \mathbf{e}_i >= 0, \quad i \in \mathscr{M} \tag{1}$$

with terminal condition

$$V_i(S, T) = P(S), \tag{2}$$

for $(S, t) \in [0, \infty) \times [0, T)$ where $P(S)$ is the payoff function, $\mathbf{V}(S, t) = (V_1(S, t), V_2(S, t), \ldots, V_m(S, t))^T$, $< \cdot, \cdot >$ is the usual inner product on $\mathbb{R}^m$ defined by

$$< \mathbf{QV}(S,t), \mathbf{e}_i >= \sum q_{il} V_l(S,t),$$

and constants r_i and σ_i are the interest rate and volatility in the ith state, respectively.

Now, we consider the change of variables $x = \log(\frac{S}{S_0})$ and $\tau = T - t$, and let $U_i(x, \tau) = V_i(S, t)$, denoted as the value of an option on the transformed space x for regime i so $U_i(x, \tau)$ satisfies the partial differential equation

$$\frac{\partial U_i}{\partial \tau} - \mathscr{R} U_i = 0, \quad i \in \mathscr{M} \tag{3}$$

with initial condition

$$U_i(x, 0) = P(S_0 e^x) =: g(x), \tag{4}$$

for $(x, \tau) \in \mathbb{R} \times (0, T]$ where

$$\mathscr{R} U_i := \frac{1}{2}\sigma_i^2 \frac{\partial^2 U_i}{\partial x^2} + \left(r_i - \frac{1}{2}\sigma_i^2\right) \frac{\partial U_i}{\partial x} - r_i U_i + < \mathbf{QU}, \mathbf{e}_i > . \tag{5}$$

For simplicity, the operator $\mathscr{R}$ is separated into the following form

$$\mathscr{R} U_i = \mathscr{D} U_i + < \mathbf{QU}, \mathbf{e}_i >, \tag{6}$$

where the differential operator $\mathscr{D}$ defined by

$$\mathscr{D}U_i := \frac{1}{2}\sigma_i^2 \frac{\partial^2 U_i}{\partial x^2} + \left(r_i - \frac{1}{2}\sigma_i^2\right)\frac{\partial U_i}{\partial x} - r_i U_i. \tag{7}$$

In order to develop a numerical scheme for partial differential equation (3), we need to impose some boundary conditions, so let the asymptotic behavior of the European call option as

$$\lim_{x\to-\infty} U_i(x,\tau) = 0, \quad \lim_{x\to\infty}[U_i(x,\tau) - S_0(e^x - e^{-r_i\tau})] = 0, \tag{8}$$

and the asymptotic behavior of the European put option is defined by

$$\lim_{x\to-\infty}[U_i(x,\tau) - S_0(e^{-r_i\tau} - e^x)] = 0, \quad \lim_{x\to\infty} U_i(x,\tau) = 0. \tag{9}$$

It is useful to mention that for numerical experiments, first we truncate the unbounded domain in $x \in (-\infty,\infty)$ direction with a bounded domain $[x_{\min}, x_{\max}]$, so for boundary conditions of European call option we have

$$U_i(x_{\min},\tau) = 0, \quad U_i(x_{\max},\tau) = S_0(e^{x_{\max}} - e^{-r_i\tau}), \tag{10}$$

and for European put option, boundary conditions are defined by

$$U_i(x_{\min},\tau) = S_0(e^{-r_i\tau} - e^{x_{\min}}), \quad U_i(x_{\max},\tau) = 0. \tag{11}$$

In the following, we will give a PDE formulation to price an American option under the regime switching model. An American option has the early exercise feature, so the optimal exercise boundary is a free boundary and separates the stopping and continuation region. Let $V_i(S,t)$ denote the fair value of an American option at time t if the asset price at that time is $S_t = S$, so $V_i(S,t)$ satisfy the following free boundary value problem

$$\begin{cases} \frac{\partial V_i(S,t)}{\partial t} + \frac{1}{2}S^2\sigma_i^2\frac{\partial^2 V_i(S,t)}{\partial S^2} + r_i S\frac{\partial V_i(S,t)}{\partial S} - r_i V_i(S,t) + < \mathbf{QV}(S,t), \mathbf{e}_i >= 0, & S > S_i^f(t) \\ V_i(S,t) = P(S), & 0 \le S \le S_i^f(t), \end{cases} \tag{12}$$

where $P(S)$ is the payoff function, and $S_i^f(t)$ for $i \in \mathscr{M}$ denote the unknown free moving exercise boundaries of the option.

For solving the free boundary problem (12), there are some techniques such as linear programming [9] or penalty methods as in e.g. [39,52] and [42]. We consider the equivalent formulation as a linear complementary problem (LCP), see e.g. [41]. To derive the equivalent LCP, first we use the change of variables $x = \log(\frac{S}{S_0})$ and $\tau = T - t$ similar to European option, and let $U_i(x,\tau) = V_i(S,t)$, denoted as the value of an option on the transformed space x for regime i, so $U_i(x,\tau)$ satisfies the following LCP

$$\begin{aligned} \frac{\partial U_i}{\partial \tau} - \mathscr{R}U_i &\ge 0, \\ U_i - g &\ge 0, \\ \left(\frac{\partial U_i}{\partial \tau} - \mathscr{R}U_i\right)(U_i - g) &= 0, \end{aligned} \tag{13}$$

for $i \in \mathscr{M}$ where $\mathscr{R}$ and g are defined by (5) and (4). LCP (13) is equipped with initial condition (4) and boundary conditions

$$\lim_{x\to-\infty} U_i(x,\tau) = 0, \quad \lim_{x\to\infty}[U_i(x,\tau) - S_0(e^x - 1)] = 0, \tag{14}$$

for call options, and boundary conditions

$$\lim_{x\to-\infty}[U_i(x,\tau)-S_0(1-e^x)]=0,\quad \lim_{x\to\infty}U_i(x,\tau)=0, \tag{15}$$

for put options. Similar to European options, boundary conditions for truncated domain for call and put options are defined by

$$U_i(x_{\min},\tau)=0,\quad U_i(x_{\max},\tau)=S_0(e^{x_{\max}}-1) \tag{16}$$

and

$$U_i(x_{\min},\tau)=S_0(1-e^{x_{\min}}),\quad U_i(x_{\max},\tau)=0, \tag{17}$$

respectively.

3 RBF-FD Approximation

Consider a spatial domain $\Omega\subset\mathbb{R}^d$ and a set of distinct points $\mathbf{X}=\{\mathbf{x}_1,\mathbf{x}_2,\ldots,\mathbf{x}_N\}$ in Ω. Also, let $\phi:\Omega\times\Omega\to\mathbb{R}$ be a kernel with the property $\phi(\mathbf{x},\mathbf{y}):=\phi(\|\mathbf{x}-\mathbf{y}\|)$ for $\mathbf{x},\mathbf{y}\in\Omega$, and $\|\cdot\|$ is the Euclidean norm. Kernels with this property known as radial functions. The RBF interpolant for a continuous target function $u:\Omega\to\mathbb{R}$ known at the nodes in $\mathbf{X}$ takes the form

$$\mathscr{I}_u(\mathbf{x})=\sum_{j=1}^{N}\lambda_j\phi(\|\mathbf{x}-\mathbf{x}_j\|). \tag{18}$$

The interpolation coefficients $\{\lambda_j\}_{j=1}^N$ are determined by collocating the interpolant $\mathscr{I}_u(\mathbf{x})$ to satisfy the interpolation condition $\mathscr{I}_u(\mathbf{x}_i)=u(\mathbf{x}_i)$ for $i=1,2,\ldots,N$. This results in a symmetric system of linear equations

$$\underbrace{\begin{pmatrix}\phi(\|\mathbf{x}_1-\mathbf{x}_1\|) & \phi(\|\mathbf{x}_1-\mathbf{x}_2\|) & \cdots & \phi(\|\mathbf{x}_1-\mathbf{x}_N\|)\\ \phi(\|\mathbf{x}_2-\mathbf{x}_1\|) & \phi(\|\mathbf{x}_2-\mathbf{x}_2\|) & \cdots & \phi(\|\mathbf{x}_2-\mathbf{x}_N\|)\\ \vdots & \vdots & \ddots & \vdots\\ \phi(\|\mathbf{x}_N-\mathbf{x}_1\|) & \phi(\|\mathbf{x}_N-\mathbf{x}_2\|) & \cdots & \phi(\|\mathbf{x}_N-\mathbf{x}_N\|)\end{pmatrix}}_{\mathbf{A}}\underbrace{\begin{pmatrix}\lambda_1\\ \lambda_2\\ \vdots\\ \lambda_N\end{pmatrix}}_{\boldsymbol{\lambda}}=\underbrace{\begin{pmatrix}u_1\\ u_2\\ \vdots\\ u_N\end{pmatrix}}_{\mathbf{u}}. \tag{19}$$

When the points in $\mathbf{X}$ are chosen to be distinct and ϕ is a positive-definite radial kernel or an order one conditionally positive-definite kernel on $\mathbb{R}^d$, the coefficient matrix $\mathbf{A}$ is guaranteed to be non-singular, see [45]. Now, assume that $u:\Omega\to\mathbb{R}$ is a differentiable function. Also, let $\mathscr{L}$ as a linear differential operator. We want to approximate $\mathscr{L}u$ at scattered grids $\mathbf{X}$ with finite-difference-style local approximations. Consider any subset of $\mathbf{X}$ denoted by $\Omega_i=\{\mathbf{x}_1,\ldots,\mathbf{x}_n\}$ containing $n<<N$ nodes which are nearest neighbors to $\mathbf{x}_i$ measured by Euclidean distance in $\mathbb{R}^d$. We refer to Ω_i as the stencil corresponding to $\mathbf{x}_i$. Approximation to $\mathscr{L}u$ at $\mathbf{x}_i$ involves a linear combination of the values of u over the stencil Ω_i of the form

$$\mathscr{L}(u(\mathbf{x}_i))\approx\sum_{j=1}^{n}w_ju(\mathbf{x}_j), \tag{20}$$

where weights $\{w_j\}_{j=1}^n$ can be computed by RBFs, so this technique known as RBF-FD. We can rewrite (20) as $\mathscr{L}(u(\mathbf{x}_i))\approx\mathbf{w}\mathbf{u}_i$, so for computing RBF-FD weights, first of all, we

prepare a local interpolant, so we have

$$\mathscr{I}_u(\mathbf{x}) = \sum_{j=1}^{n} \lambda_j \phi(\|\mathbf{x} - \mathbf{x}_j\|), \tag{21}$$

and its matrix-vector form is $\mathbf{A}_i \lambda = \mathbf{u}_i$, where $\mathbf{A}_i$ and $\mathbf{u}_i$ are local distance matrix and known data corresponding to stencil of $\mathbf{x}_i$, respectively. Unknown coefficients λ_j are determined by $\lambda = \mathbf{A}_i^{-1}\mathbf{u}_i$. Now, we apply the differentiation operator $\mathscr{L}$ to the both side of (21), then we have

$$\mathscr{L}(\mathscr{I}_u(\mathbf{x})) = \sum_{j=1}^{n} \lambda_j \mathscr{L}(\phi(\|\mathbf{x} - \mathbf{x}_j\|)). \tag{22}$$

Now, by collocating (22) at $\mathbf{x}_i$ and writing matrix-vector form, we derive

$$\mathscr{L}(u(\mathbf{x}_i)) = \mathscr{L}\Phi(\mathbf{x}_i)\lambda = \mathscr{L}\Phi(\mathbf{x}_i)\mathbf{A}_i^{-1}\mathbf{u}_i. \tag{23}$$

where $\mathscr{L}\Phi(\mathbf{x}_i) = [\mathscr{L}\phi(\|\mathbf{x}_i - \mathbf{x}_1\|), \mathscr{L}\phi(\|\mathbf{x}_i - \mathbf{x}_2\|), \ldots, \mathscr{L}\phi(\|\mathbf{x}_i - \mathbf{x}_n\|)]$. By comparing (20) with (23), we conclude $\mathbf{w} = \mathscr{L}\Phi(\mathbf{x}_i)\mathbf{A}_i^{-1}$.

The global RBF method for deriving differentiation matrix needs $O(N^3)$ operations, and leads to a dense matrix, but in RBF-FD method for each stencil, we need $O(n^3)$ operations and there are N such stencils, so that the total cost of computing is $O(n^3 N)$, although we do not take into account the cost of determining the stencil grids. Since $n << N$ and n is fixed as N increases, so that the total cost will be $O(N)$. For computing weights, we need to compute the inverse of local distance matrix of order $n \times n$ for each stencil, and since distance matrix depends only on distance of grid points, in uniform grids which we use in this study, we only need to compute the inverse of local distance matrix once. Also, since computing differentiation matrix for each stencil is independent to other stencils, so parallel algorithms can be employed to increase the efficiency of RBF-FD method in high dimensional problems and adaptive algorithms.

4 Spatial Discretization

For numerical techniques, we replace the unbounded domain $\{(x, \tau) \mid x \in \mathbb{R}, \tau \in (0, T]\}$ with a bounded one $[x_{\min}, x_{\max}] \times (0, T]$ where the values $x_{\min}$ and $x_{\max}$, will be chosen based on standard financial arguments, such that the error caused by truncating the solution domain is negligible. Let $X = \{x_0, x_1, \ldots, x_N\} \subset [x_{\min}, x_{\max}]$ such that $x_{\min} = x_0 < x_1 < \cdots < x_N = x_{max}$, and for each point x_j, we choose an influence domain $X_j = \{x_1, x_2, \ldots, x_n\} \subset X$ which contains a local region formed by the n closest neighboring interpolation points to x_j. Local RBF interpolant for each regime is defined by

$$U_i(x, \tau) \approx \widetilde{U}_i(x, \tau) = \sum_{k=1}^{n} \lambda_k \phi(\|x - x_k\|) \tag{24}$$

where unknown $\{\lambda_k\}_{k=1}^n$ are determined by imposing the interpolation conditions and solving linear system of equations $\Phi^j \lambda^j = \widetilde{U}_i^j$, where $\Phi^j = [\phi(\|x_i - x_k\|)]_{1 \le i,k \le n}$, $\lambda^j = [\lambda_1, \lambda_2, \ldots, \lambda_n]^T$ and $\widetilde{U}_i^j = [\widetilde{U}_i(x_1, \tau), \widetilde{U}_i(x_2, \tau), \ldots, \widetilde{U}_i(x_n, \tau)]^T$, regarding to this fact that Φ^j is invertible, so we have $\lambda^j = (\Phi^j)^{-1}\widetilde{U}_i^j$.

For each interior point $x_j \in X$ we apply differential operator (7) to the local interpolant (24), so we have

$$\mathscr{D}\widetilde{U}_i(x_j,\tau) = \sum_{k=1}^{n} \lambda_k \mathscr{D}\phi(\|x_j - x_k\|) =: \Psi_i^j \widetilde{U}_i^j \tag{25}$$

where similar to previous section

$$\Psi_i^j = [\mathscr{D}\phi(\|x_j - x_1\|), \mathscr{D}\phi(\|x_j - x_2\|), \ldots, \mathscr{D}\phi(\|x_j - x_n\|)](\Phi^j)^{-1}. \tag{26}$$

Now, by substituting local interpolant (24) and (25) in (3), locally we have

$$\frac{\partial \widetilde{U}_i^j}{\partial \tau} = \Psi_i^j \widetilde{U}_i^j + < \mathbf{Q}\widetilde{\mathbf{U}}^j, \mathbf{e}_i >, \quad i \in \mathscr{M} \tag{27}$$

where $\widetilde{\mathbf{U}}^j = [\widetilde{U}_1(x_j,\tau), \widetilde{U}_2(x_j,\tau), \ldots, \widetilde{U}_m(x_j,\tau)]^T$.

The above equation in the local form is equivalent to the following global form

$$\frac{\partial \widetilde{U}_i}{\partial \tau} = \Psi_i \widetilde{U}_i + < \mathbf{Q}\widetilde{\mathbf{U}}, \mathbf{e}_i >, \quad i \in \mathscr{M} \tag{28}$$

where $\frac{\partial \widetilde{U}_i}{\partial \tau} = [\frac{\partial \widetilde{U}_i(x_1,\tau)}{\partial \tau}, \frac{\partial \widetilde{U}_i(x_2,\tau)}{\partial \tau}, \ldots, \frac{\partial \widetilde{U}_i(x_{N-1},\tau)}{\partial \tau}]^T$, $\widetilde{U}_i = [\widetilde{U}_i(x_1,\tau), \widetilde{U}_i(x_2,\tau), \ldots, \widetilde{U}_i(x_{N-1},\tau)]^T$ and Ψ_i is the mapping of Ψ_i^j from local to global by inserting zeros in the proper locations. We can rewrite system of equations (28) as

$$\frac{\partial \widetilde{\mathbf{U}}}{\partial \tau} = \mathbf{A}_I \widetilde{\mathbf{U}} \tag{29}$$

where $\mathbf{A}_I = blkdiag(\Psi_1, \Psi_2, \ldots, \Psi_m) + \mathbf{Q} \otimes I$, $\widetilde{\mathbf{U}} = [\widetilde{U}_1, \widetilde{U}_2, \ldots, \widetilde{U}_m]$ and *blkdiag* and $\otimes$ mean block diagonal and tensor product, respectively.

Similarly, for each boundary point $x_j \in X$, we can choose an influence domain X_j, and let $\mathscr{B}$ as a boundary operator, so we have

$$\mathscr{B}\widetilde{U}_i(x_j,\tau) = \sum_{k=1}^{n} \lambda_k \mathscr{B}\phi(\|x_j - x_k\|) =: \Upsilon_i^j \widetilde{U}_i^j \tag{30}$$

where

$$\Upsilon_i^j = [\mathscr{B}\phi(\|x_j - x_1\|), \mathscr{B}\phi(\|x_j - x_2\|), \ldots, \mathscr{B}\phi(\|x_j - x_n\|)](\Phi^j)^{-1}, \tag{31}$$

and in this paper, we consider Dirichlet boundary condition, so operator $\mathscr{B}$ is the identity operator. Similar to what we have done for interior points, we can extend the local system to the global form as

$$\Upsilon_i \widetilde{U}_i = G_i, \quad i \in \mathscr{M} \tag{32}$$

where Υ_i is the extension of Υ_i^j similar to the mapping of Ψ_i^j to Ψ_i, and G_i is related to Dirichlet boundary condition.

To impose system of boundary conditions (32) to (29), for each block of $\mathbf{A}_I$ corresponding to each regime, we insert two rows related to boundary grids derived in (32). Finally, we conclude the following semidiscrete system of equations

$$\frac{\partial \widetilde{\mathbf{U}}}{\partial \tau} = \mathbf{A}\widetilde{\mathbf{U}}, \tag{33}$$

where $\mathbf{A}$ is the discretization matrix corresponding to interior and boundary points.

Similarly, for LCP (13), we get the following semidiscrete system of equations

$$\begin{aligned} \frac{\partial \widetilde{\mathbf{U}}}{\partial \tau} - \mathbf{A}\widetilde{\mathbf{U}} &\geq 0, \\ \widetilde{\mathbf{U}} - g &\geq 0 \\ \left(\frac{\partial \widetilde{\mathbf{U}}}{\partial \tau} - \mathbf{A}\widetilde{\mathbf{U}}\right)^T (\widetilde{\mathbf{U}} - g) &= 0. \end{aligned} \tag{34}$$

5 Time Discretization

Let $\triangle\tau = \frac{T}{M}$ with integer $M \geq 1$ be a given time step, and let temporal grid points $\tau_k = k\triangle\tau$ for $0 \leq k \leq M$. To apply time discretization for (33), we employ an often used scheme known as the θ-method, with parameter $\theta \in [0, 1]$. The choices $\theta = \frac{1}{2}$ and $\theta = 1$ represent, respectively, the well-known Crank–Nicolson and backward Euler methods. Now, let $\widetilde{\mathbf{U}}^k \approx \widetilde{\mathbf{U}}(\tau_k)$, so for European option we have

$$\frac{\widetilde{\mathbf{U}}^{k+1} - \widetilde{\mathbf{U}}^k}{\triangle\tau} = \theta\mathbf{A}\widetilde{\mathbf{U}}^{k+1} + (1-\theta)\mathbf{A}\widetilde{\mathbf{U}}^k, \quad for \quad 0 \leq k \leq M-1, \tag{35}$$

then, linear system of equations

$$(I - \theta\triangle\tau\mathbf{A})\widetilde{\mathbf{U}}^{k+1} = (I + (1-\theta)\triangle\tau\mathbf{A})\widetilde{\mathbf{U}}^k, \quad for \quad 0 \leq k \leq M-1, \tag{36}$$

with initial condition $\widetilde{\mathbf{U}}^0 = g$ is derived.

One of the sources of error can arise when we use initial function (4) at the RBF-FD grid points, since this function is discontinuous in their first derivatives. A useful notion in the implementation of numerical method is that the value of a function on a grid represents average value of the function over the surrounding grids rather than its value sampled at each grid point [37] by

$$g(x_i) \approx \frac{1}{h}\int_{x_i-\frac{h}{2}}^{x_i+\frac{h}{2}} g(x)dx,$$

and this makes the payoff function smooth at the strike price S_0, and we use this technique to improve the accuracy of RBF-FD numerical method especially near the strike price.

For American options, the most commonly used method for solving (34) is the projected successive over relaxation (PSOR) method [27], but it is rather inefficient for finer space discretization. In this paper, we propose time discretization scheme based on operator splitting which was introduced by Ikonen and Toivanen in [28] to evaluate the price of the American put option under the Black–Scholes model. The operator splitting method is based on the formulation with an auxiliary vector Λ as follow

$$\begin{aligned} \frac{\partial \widetilde{\mathbf{U}}}{\partial \tau} - \mathbf{A}\widetilde{\mathbf{U}} &= \Lambda, \\ \Lambda &\geq 0 \\ \widetilde{\mathbf{U}} - g &\geq 0 \\ (\Lambda)^T(\widetilde{\mathbf{U}} - g) &= 0. \end{aligned} \tag{37}$$

By using the θ-method for time discretization of the semidiscrete system of equations (37), we define approximations $\widetilde{\mathbf{U}}^k \approx \widetilde{\mathbf{U}}(\tau_k)$ successively for $k = 0, 1, \ldots, M-1$ by

$$\begin{aligned}(I - \theta\triangle\tau\mathbf{A})\widetilde{\mathbf{U}}^{k+1} &= (I + (1-\theta)\triangle\tau\mathbf{A})\widetilde{\mathbf{U}}^k + \triangle\tau\Lambda^{k+1}\\ \Lambda^{k+1} &\geq 0\\ \widetilde{\mathbf{U}}^{k+1} - g &\geq 0\\ (\Lambda^{k+1})^T(\widetilde{\mathbf{U}}^{k+1} - g) &= 0.\end{aligned} \tag{38}$$

To apply operator splitting method for solving (38), each time step $[\tau_k, \tau_{k+1}]$ is splitted into two parts. First, an intermediate solution $\underline{\widetilde{\mathbf{U}}}^{k+1}$ for $k = 0, 1, \ldots, M-1$ is determined by solving the modified system of linear equations

$$(I - \theta\triangle\tau\mathbf{A})\underline{\widetilde{\mathbf{U}}}^{k+1} = (I + (1-\theta)\triangle\tau\mathbf{A})\widetilde{\mathbf{U}}^k + \triangle\tau\Lambda^k, \tag{39}$$

where $\widetilde{\mathbf{U}}^0 = g$, and the vector $\underline{\Lambda}^{k+1}$ is given at the start of each time step.

The second stage is concerned with determining the approximation solutions $\widetilde{\mathbf{U}}^{k+1}$ and Λ^{k+1} on the subinterval $[\tau_k, \tau_{k+1}]$ by solving the problem

$$\widetilde{\mathbf{U}}^{k+1} - \underline{\widetilde{\mathbf{U}}}^{k+1} = \triangle\tau(\Lambda^{k+1} - \Lambda^k), \tag{40}$$

with two inequality constraints and one equality constraint

$$\Lambda^{k+1} \geq 0, \quad \widetilde{\mathbf{U}}^{k+1} - g \geq 0, \quad (\Lambda^{k+1})^T(\widetilde{\mathbf{U}}^{k+1} - g) = 0.$$

Values $\widetilde{\mathbf{U}}^{k+1}$ and Λ^{k+1} can be determined very fast at each spatial grid point independently with the formulas

$$\widetilde{\mathbf{U}}^{k+1} = \max\{g, \underline{\widetilde{\mathbf{U}}}^{k+1} - \triangle\tau\Lambda^k\}, \quad \Lambda^{k+1} = \Lambda^k + \frac{\widetilde{\mathbf{U}}^{k+1} - \underline{\widetilde{\mathbf{U}}}^{k+1}}{\triangle\tau}. \tag{41}$$

6 Stability Analysis

In this section, to apply RBF-FD discretization for operator $\mathscr{D}$ defined in (7), we show how we can derive the exact RBF-FD formulas for first and second derivatives. In the following, we use multiquadrics as RBFs, defined by

$$\phi(\|\mathbf{x} - \mathbf{y}\|) = \sqrt{\varepsilon^2 + (\|\mathbf{x} - \mathbf{y}\|)^2}, \tag{42}$$

where $\|\cdot\|$ is the Euclidean norm and ε is the shape parameter. Also, we assume that the grid points in x direction are equidistance with step size h and $n = 3$ is the number of grids in influence domain which are closest neighboring interpolation points to x_j. Also, in continue we derive the stability analysis of RBF-FD combined with θ method for full discretized system of equations (36). In this system of equations, $\mathbf{A}$ is an sparse discretized matrix derived by RBF-FD discretization for operator $\mathscr{R}$ defined by (5) which contains the differential operator $\mathscr{D}$ defined by (7) and non-differential part $< \mathbf{QU}, \mathbf{e}_i >$.

So, the first derivative of $U_i(x, \tau)$ at $x = x_j$ is approximated by

$$\frac{\partial U_i}{\partial x}(x_j, \tau) = \alpha_{j-1}U_i(x_j - h, \tau) + \alpha_j U_i(x_j, \tau) + \alpha_{j+1}U_i(x_j + h, \tau), \tag{43}$$

so, by substituting function $U_i(x, \tau)$ by multiquadrics radial basis functions centered at $x_j - h$, x_j, and $x_j + h$, the unknown coefficients α_{j-1}, α_j and α_{j+1} are derived by solving

a 3×3 linear system of equations, then we have

$$\alpha_{j-1} = -\alpha_{j+1} = -\frac{1}{4h}\frac{1+\sqrt{1+\frac{4h^2}{\varepsilon^2}}}{\sqrt{1+\frac{h^2}{\varepsilon^2}}}, \qquad \alpha_j = 0. \tag{44}$$

In the numerical experiments, we assume $\varepsilon \gg h$, so we get [6]

$$\alpha_{j-1} = -\alpha_{j+1} = -\frac{1}{2h}\left(1+\frac{h^2}{2\varepsilon^2}\right), \qquad \alpha_j = 0, \tag{45}$$

and since our grid points are equidistance, so for all j, we let

$$\alpha = \alpha_{j+1} = \frac{1}{2h}\left(1+\frac{h^2}{2\varepsilon^2}\right), \quad \alpha_{j-1} = -\alpha, \quad \alpha_j = 0. \tag{46}$$

Now, for second derivative of $U_i(x,\tau)$ at $x = x_j$ let

$$\frac{\partial^2 U_i}{\partial x^2}(x_j,\tau) = \beta_{j-1}U_i(x_j-h,\tau) + \beta_j U_i(x_j,\tau) + \beta_{j+1}U_i(x_j+h,\tau), \tag{47}$$

so, the unknown coefficients β_{j-1}, β_j and β_{j+1} are derived by

$$\begin{aligned}
\beta_{j-1} = \beta_{j+1} &= \frac{2+\left(\frac{h^2}{\varepsilon^2}+2\right)\sqrt{1+\frac{4h^2}{\varepsilon^2}}+\frac{5h^2}{\varepsilon^2}+\frac{2h^4}{\varepsilon^4}}{4h^2\left(1+\frac{h^2}{\varepsilon^2}\right)^{\frac{3}{2}}},\\
\beta_j &= -\frac{2+\left(\frac{h^2}{\varepsilon^2}+2\right)\sqrt{1+\frac{4h^2}{\varepsilon^2}}+\frac{3h^2}{\varepsilon^2}}{2h^2\left(1+\frac{h^2}{\varepsilon^2}\right)}.
\end{aligned} \tag{48}$$

Also, if we assume $\varepsilon \gg h$, and the gride points are equidistance, then we have [6]

$$\beta_2 = \beta_{j-1} = \beta_{j+1} = \frac{1}{h^2}\left(1+\frac{h^2}{\varepsilon^2}\right), \quad \beta_1 = \beta_j = -\frac{2}{h^2}\left(1+\frac{h^2}{\varepsilon^2}\right). \tag{49}$$

Now, by substituting the above first and second derivative approximations in operator $\mathscr{D}$ we get the following differential matrix

$$\mathbf{D} = \frac{1}{2}\sigma_i^2\begin{pmatrix} \beta_1 & \beta_2 & & & \\ \beta_2 & \beta_1 & \beta_2 & & \\ & \ddots & \ddots & \ddots & \\ & & \beta_2 & \beta_1 & \beta_2 \\ & & & \beta_2 & \beta_1 \end{pmatrix} + \left(r_i - \frac{1}{2}\sigma_i^2\right)\begin{pmatrix} 0 & \alpha & & & \\ -\alpha & 0 & \alpha & & \\ & \ddots & \ddots & \ddots & \\ & & -\alpha & 0 & \alpha \\ & & & -\alpha & 0 \end{pmatrix} - r_i I, \tag{50}$$

finally,

$$\mathbf{D} = tridiag\left(\frac{1}{2}\sigma_i^2\beta_2 - \left(r_i - \frac{1}{2}\sigma_i^2\right)\alpha\ ,\ \frac{1}{2}\sigma_i^2\beta_1 - r_i\ ,\ \frac{1}{2}\sigma_i^2\beta_2 + \left(r_i - \frac{1}{2}\sigma_i^2\right)\alpha\right), \tag{51}$$

where *tridiag* means tridiagonal matrix.

Definition 1 [49]. A real $n \times n$ matrix $A = [a_{i,j}]$ is a Z-matrix if $a_{i,j} \le 0$ for all $i \ne j$.

Definition 2 [43]. A real $n \times n$ matrix $A = [a_{i,j}]$ with $a_{i,j} \le 0$ for all $i \ne j$ is an M-matrix if A is nonsingular and $A^{-1} \ge 0$ (means all elements of A^{-1} must be nonnegative).

In this paper, our mean about convergence of matrix A is $\rho(A) < 1$ where $\rho(A)$ denotes the spectral radius of A.

Lemma 1 *Let $A = [a_{i,j}]$ be an $n \times n$ Z-matrix, then the following statements are equivalent:*

1. *A is a nonsingular M-matrix.*
2. *There exists a vector $v > 0$ such that $Av > 0$.*
3. *$A + I$ is nonsingular, and $G = (A + I)^{-1}(A - I)$ is convergent.*

Proof [7] □

Regarding to Lemma 1, if in the second statement, we let $v = \mathbf{1}$ as a vector with all elements one, and also let matrix $A = [a_{i,j}]$ with $a_{i,j} \leq 0$ for all $i \neq j$ and $a_{i,i} > 0$, then $Av > 0$ is equivalent with diagonally dominance of matrix A.

Theorem 1 *Matrix $-\mathbf{D}$ is a nonsingular M-matrix if $\left|1 - \frac{2r_i}{\sigma_i^2}\right| \leq \frac{\beta_2}{\alpha} \approx O(\frac{1}{h})$ for all $i \in \mathscr{M}$ where α and β_2 are defined by (46) and (49).*

Proof To show matrix $-\mathbf{D}$ is a nonsingular M-matrix, it is sufficient to show that matrix $-\mathbf{D}$ is diagonal dominant with positive diagonal entries, and nonpositive off-diagonal entries. Since r_i and σ_i are positive for all $i \in \mathscr{M}$ and β_1 is negative, so $r_i - \frac{1}{2}\sigma_i^2\beta_1 > 0$ which are the diagonal entries of matrix $-\mathbf{D}$. For off-diagonal entries of matrix $-\mathbf{D}$, we should prove

$$\frac{1}{2}\sigma_i^2\beta_2 - \left(r_i - \frac{1}{2}\sigma_i^2\right)\alpha \geq 0, \quad \frac{1}{2}\sigma_i^2\beta_2 + \left(r_i - \frac{1}{2}\sigma_i^2\right)\alpha \geq 0, \tag{52}$$

so by using assumption

$$\left|1 - \frac{2r_i}{\sigma_i^2}\right| \leq \frac{\beta_2}{\alpha},$$

inequalities (52) are satisfied.

Now, we show that matrix $-\mathbf{D}$ is diagonal dominant. Since diagonal entries of $-\mathbf{D}$ are positive and off-diagonal entries are nonpositive, so it is sufficient to show sum of all nonzero entries of $-\mathbf{D}$ in each row is positive, and equivalently for matrix $\mathbf{D}$, we should prove that sum of all nonzero entries of $\mathbf{D}$ in each row is negative.

For the first row of $\mathbf{D}$, we must show that sum of nonzero entries $\frac{1}{2}\sigma_i^2(\beta_1 + \beta_2) + (r_i - \frac{1}{2}\sigma_i^2)\alpha - r_i$ is negative. We know $2\beta_2 + \beta_1 = 0$, so by substitute $\beta_2 + \beta_1 = -\beta_2$, we get

$$\frac{1}{2}\sigma_i^2(\beta_1 + \beta_2) + \left(r_i - \frac{1}{2}\sigma_i^2\right)\alpha - r_i = -\frac{1}{2}\sigma_i^2\beta_2 + \left(r_i - \frac{1}{2}\sigma_i^2\right)\alpha - r_i$$

and by using inequalities (52), $-\frac{1}{2}\sigma_i^2(\beta_2) + (r_i - \frac{1}{2}\sigma_i^2)\alpha \leq 0$, and $-r_i < 0$, therefore $-\frac{1}{2}\sigma_i^2\beta_2 + (r_i - \frac{1}{2}\sigma_i^2)\alpha - r_i < 0$.

For middle rows of $\mathbf{D}$ with three nonzero entries, sum of all nonzero entries of $\mathbf{D}$ in each row is

$$\sigma_i^2\beta_2 + \frac{1}{2}\sigma_i^2\beta_1 - r_i = \frac{1}{2}\sigma_i^2(2\beta_2 + \beta_1) - r_i,$$

since $2\beta_2 + \beta_1 = 0$ and $r_i > 0$ for all $i \in \mathscr{M}$, so it is clear that sum of all nonzero entries of $\mathbf{D}$ in each row for middle rows is negative.

For the last row of $\mathbf{D}$, we must prove that $\frac{1}{2}\sigma_i^2(\beta_1+\beta_2)-(r_i-\frac{1}{2}\sigma_i^2)\alpha-r_i<0$. Similar to the first row of $\mathbf{D}$, we have

$$\frac{1}{2}\sigma_i^2(\beta_1+\beta_2)-\left(r_i-\frac{1}{2}\sigma_i^2\right)\alpha-r_i=-\frac{1}{2}\sigma_i^2\beta_2-\left(r_i-\frac{1}{2}\sigma_i^2\right)\alpha-r_i$$

and by using inequalities (52), $-\frac{1}{2}\sigma_i^2(\beta_2)-(r_i-\frac{1}{2}\sigma_i^2)\alpha\leq 0$, and $-r_i<0$, therefore $-\frac{1}{2}\sigma_i^2\beta_2-(r_i-\frac{1}{2}\sigma_i^2)\alpha-r_i<0$ is satisfied, and this completes the proof for the diagonally dominant property. □

Remark 1 In Theorem 1, if condition $\left|1-\frac{2r_i}{\sigma_i^2}\right|\leq\frac{\beta_2}{\alpha}$ is satisfied, then we can derive matrix $-\mathbf{D}$ is a nonsingular M-matrix. For a fixed value of shape parameter ε, and small enough value for step size h, it is easy to see that $\frac{\beta_2}{\alpha}\to\infty$, and this limit value show that for small values of h, this assumption is easily available.

Remark 2 With properties of matrix $\mathbf{Q}$ given in Sect. 2, it is easy to derive that matrix $-\mathbf{Q}$ is diagonal dominant with positive diagonal entries, and nonpositive off-diagonal entries, so Lemma 1 grantees that matrix $-\mathbf{A}=-\mathbf{D}-\mathbf{Q}$ is a nonsingular M-matrix where matrix $\mathbf{A}$ is defined by (33) as the discretization matrix .

Remark 3 Since $-\mathbf{A}$ is an M-matrix and nonsingular, so $-\theta\triangle\tau\mathbf{A}$ is also an M-matrix and nonsingular. By using Lemma 1, it is easy to derive that $(I-\theta\triangle\tau\mathbf{A})$ is nonsingular, then linear system of equations (36) has a unique solution.

For discussion about the stability of RBF-FD method, let $e^k=\widetilde{\mathbf{U}}_{ex}^k-\widetilde{\mathbf{U}}_{ap}^k$ as a small perturbation at kth time level, where $\widetilde{\mathbf{U}}_{ex}^k$ is the exact and $\widetilde{\mathbf{U}}_{ap}^k$ is the approximate solution of (36). The equation for error e^{k+1} can be written as $e^{k+1}=\mathbf{G}e^k$, where $\mathbf{G}=(I-\theta\triangle\tau\mathbf{A})^{-1}(I+(1-\theta)\triangle\tau\mathbf{A})$. The numerical scheme will be stable if as $k\to\infty$, the error $e^k\to 0$. This can be ensured provided $\rho(\mathbf{G})<1$, where $\rho(\mathbf{G})$ denote the spectral radius of $\mathbf{G}$. For the case of the Crank–Nicolson scheme ($\theta=\frac{1}{2}$), and regarding to the Lemma 1, the condition $\rho(\mathbf{G})<1$ and convergence of $\mathbf{G}$ is always satisfied provided $-\mathbf{A}$ is a nonsingular M-matrix, then this shows that scheme is stable.

7 Numerical Results

In this section, we carry out some numerical experiments to evaluate the prices of European and American options under the regime switching model. The truncated domain of the log price for all examples are chosen to be $[x_{\min},x_{\max}]=[-1.5,1.5]$ except example 3 for $T=10$ which we let $[x_{\min},x_{\max}]=[-2.5,2.5]$, and as RBF for spatial discertization, we select the multiquadric radial basis function defined by (42) with $\varepsilon=0.5$ for all American and European options, and we choose $n=3$ as number of local nodes in each stencil. Also, all experiments are performed on a PC with a 3.6 GHz Corei3 processor.

For European option under the regime switching model, there exists an analytical solution, so *Error* in tables refers to the difference between analytical and approximate solutions, but for American option, analytical solution is not available, so in tables, *Error* refers to the difference between successive numerical solutions following mesh refinements, given by

$$Error=\left|\widetilde{U}_i(\triangle x,\triangle\tau)-\widetilde{U}_i\left(\frac{\triangle x}{2},\frac{\triangle\tau}{2}\right)\right|,$$

Table 1 Absolute errors for European call option values derived by RBF-FD method for $N = 512$ and $M = 256$, a numerical PDE algorithm reported in [10], tree method presented in [33] and pseudospectral (PS) method [15] at different stock prices with parameter set of Example 1

S	Regime 1				Regime 2			
	RBF-FD	[10]	Tree [33]	PS [15]	RBF-FD	[10]	Tree [33]	PS [15]
94	3.1e−04	4.1e−03	8.0e−04	4.1e−04	2.3e−05	9.9e−03	8.0e−04	8.3e−04
96	2.0e−04	5.7e−03	5.0e−04	5.0e−04	4.4e−06	1.1e−02	1.0e−04	8.7e−04
98	3.4e−05	6.9e−03	1.0e−03	6.5e−04	1.6e−04	1.2e−02	1.0e−04	1.0e−03
100	8.4e−05	7.7e−04	1.8e−03	7.6e−04	2.9e−04	1.3e−02	2.1e−03	1.2e−03
102	2.0e−04	8.1e−03	1.4e−03	8.7e−04	4.2e−04	1.3e−02	2.0e−04	1.3e−03
104	3.8e−04	8.2e−03	1.4e−03	1.1e−03	4.8e−04	1.4e−02	1.4e−03	1.4e−03
106	5.3e−04	7.9e−03	1.5e−03	1.2e−03	6.1e−04	1.3e−02	4.0e−04	1.5e−03
time(s)	0.213			32.04	0.213			32.04
cond	8.113				8.113			

where $\triangle x = \frac{x_{\max} - x_{\min}}{N}$ and $\triangle \tau = \frac{T}{M}$ are space and time step sizes, respectively. Also, *Ratio* denotes the $\log_2$ ratio of errors defined by

$$Ratio = \log_2 \left(\left| \frac{\widetilde{U}_i(\triangle x, \triangle \tau) - \widetilde{U}_i(\frac{\triangle x}{2}, \frac{\triangle \tau}{2})}{\widetilde{U}_i\left(\frac{\triangle x}{2}, \frac{\triangle \tau}{2}\right) - \widetilde{U}_i\left(\frac{\triangle x}{4}, \frac{\triangle \tau}{4}\right)} \right| \right).$$

Example 1 In this example, we consider European call option under the regime switching model with parameters

$$\begin{pmatrix} r_1 \\ r_2 \end{pmatrix} = \begin{pmatrix} 0.05 \\ 0.05 \end{pmatrix}, \quad \begin{pmatrix} \sigma_1 \\ \sigma_2 \end{pmatrix} = \begin{pmatrix} 0.15 \\ 0.25 \end{pmatrix}, \quad \mathbf{Q} = \begin{pmatrix} -0.5 & 0.5 \\ 0.5 & -0.5 \end{pmatrix}, \quad T = 1, \quad S_0 = 100$$

chosen from [33]. An explicit closed-form formula for the arbitrage-free price of the European call option is available in [21]. In Table 1, for a list of stock prices, absolute errors for RBF-FD method developed in the present paper for $N = 512$ and $M = 256$, a numerical PDE algorithm proposed in [10], tree method presented in [33] and pseudospectral (PS) method [15] by using Chebfun package are reported for comparison. Also, at the button of Table 1, *time(s)* and *cond* stand CPU time in second and condition number of arisen linear system, respectively.

Example 2 In this example, we consider the following parameters

$$\begin{pmatrix} r_1 \\ r_2 \end{pmatrix} = \begin{pmatrix} 0.1 \\ 0.05 \end{pmatrix}, \quad \begin{pmatrix} \sigma_1 \\ \sigma_2 \end{pmatrix} = \begin{pmatrix} 0.8 \\ 0.3 \end{pmatrix}, \quad \mathbf{Q} = \begin{pmatrix} -6 & 6 \\ 9 & -9 \end{pmatrix}, \quad T = 1, \quad S_0 = 9$$

to price an American put option with two regimes. For different number of spatial grids and time steps, results are derived by RBF-FD method including option *Price*, *Error*, *Ratio* and CPU *time(s)* and presented in Table 2.

For more investigation about the efficiency of RBF-FD method, we define the following maximum error

$$= \max_{x_{\min} \le x_j \le x_{\max}} \left| \widetilde{U}_i(x_j, T) - \widetilde{U}_i^{ref}(x_j, T) \right| \tag{53}$$

Table 2 Numerical results of RBF-FD method for American put option with two regimes for Example 2

M	N	Regime 1			Regime 2			
		Price	Error	Ratio	Price	Error	Ratio	Time (s)
50	50	1.9699970			1.8813124			0.010
100	100	1.9714882	1.5e−03		1.8821686	8.6e−04		0.041
200	200	1.9718763	3.9e−04	1.942	1.8823926	2.2e−04	1.935	0.103
400	400	1.9719660	9.0e−05	2.113	1.8824414	4.9e−05	2.197	0.308
800	800	1.9719838	1.8e−05	2.333	1.8824491	7.8e−06	2.651	0.853

Table 3 Maximum error and ratio for different number of spatial grids N and time steps M of RBF-FD method for American put option with two regimes for Example 2

M	N	Regime 1		Regime 2	
		Max error	Ratio	Max error	Ratio
50	50	7.3e−03		6.5e−03	
100	100	1.8e−03	1.998	1.6e−03	2.009
200	200	4.3e−04	2.100	3.7e−04	2.123
400	400	9.0e−05	2.246	7.7e−05	2.282
800	800	1.5e−05	2.523	1.5e−05	2.287

Table 4 American put option prices computed by RBF-FD with $\triangle x = \triangle \tau = 0.01$, FF-expl [16], ETD-CN [30] and Tree [33] methods for two regimes for Example 2

S	Regime 1				Regime 2			
	RBF-FD	FF-expl	ETD-CN	Tree	RBF-FD	FF-expl	ETD-CN	Tree
6	3.4143		3.4196	3.4144	3.3507		3.3563	3.3503
7.5	2.5842		2.5886	2.5844	2.5033		2.5077	2.5028
9	1.9718	1.9713	1.9756	1.9722	1.8825	1.8817	1.8859	1.8819
10.5	1.5185	1.5177	1.5213	1.5186	1.4274	1.4265	1.4301	1.4267
12	1.1803	1.1796	1.1825	1.1803	1.0924	1.0915	1.0945	1.0916

where $x_j = x_{\min} + j\triangle x$ and $\triangle x = \frac{x_{\max} - x_{\min}}{300}$ and $j = 0, 1, \ldots, 300$. In the case of the American option the exact solution is not available. Therefore, in the definition of maximum error, we use a very accurate solution obtained by the RBF-FD approximation with a very large number of grid points $N = 2400$ and time steps $M = 2400$ as $\widetilde{U}_i^{ref}$. For different number of spatial grids N and time steps M, results are derived and presented in Table 3.

Our solutions prepared by RBF-FD method are compared with other methods in Table 4 which contains option prices for different values of asset price S computed by front-fixing explicit method (FF-expl) [16], the exponential time differencing Crank–Nicolson scheme (ETD-CN) [30], and the binomial tree approach (Tree) developed in [33]. The solutions derived by RBF-FD method with $\triangle x = \triangle \tau = 0.01$, also condition number of arisen linear system is 47.601, and CPU time is 0.058 s. It is important to mention that the reported CPU times for the experiments do not include the setup cost for the computations of the differentiation matrices. From Table 4, we derive that our option prices are in line with those obtained by different techniques.

An option's price can be influenced by a number of factors. To become a successful option trader, it is essential to understand what factors influence the price of an option, which requires

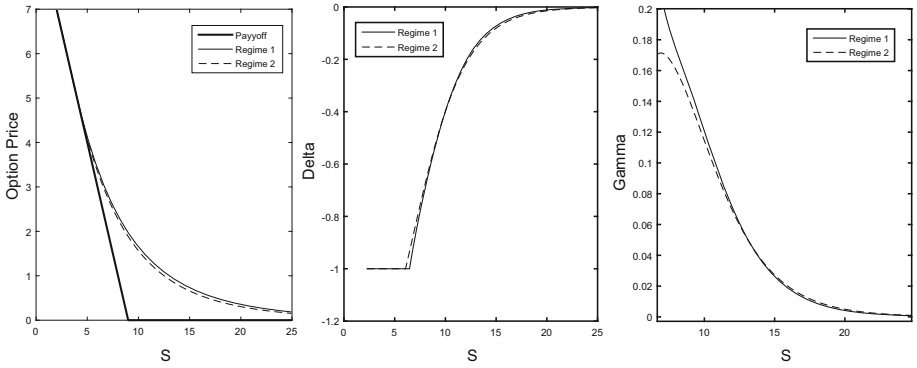

Fig. 1 Today's American put price, Delta and Gamma values for RBF-FD method with parameters as provided in Example 2

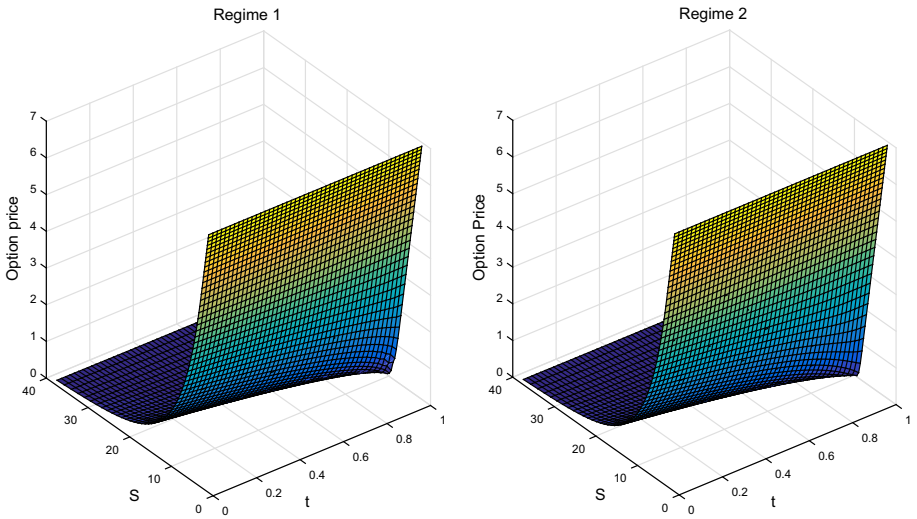

Fig. 2 The option price surface for two regimes derived by RBF-FD method with parameters as provided in Example 2

learning about the Greeks. Figure 1 displays the option values, the Delta and the Gamma functions known as Greeks. The plot shows that the option values and Greeks are very stable and there is no oscillation at or around the strike price. This figure shows that Greeks are efficiently evaluated using proposed method. Also, in Fig. 2, we plot option price surfaces that are obtained with RBF-FD method for two different regimes.

Example 3 In this example, we consider the following parameters

$$\begin{pmatrix} r_1 \\ r_2 \end{pmatrix} = \begin{pmatrix} 0.05 \\ 0.05 \end{pmatrix}, \quad \begin{pmatrix} \sigma_1 \\ \sigma_2 \end{pmatrix} = \begin{pmatrix} 0.3 \\ 0.4 \end{pmatrix}, \quad \mathbf{Q} = \begin{pmatrix} -3 & 3 \\ 2 & -2 \end{pmatrix}, \quad S_0 = 10,$$

$T = 1$ and $T = 10$ adapted by [2] which in it authors compare iterated optimal stopping (IOS) and local policy iteration (LPI) methods to evaluate option price of an American case with regime switching model. Option prices and CPU times for different time steps and grid

Table 5 American put option values derived from RBF-FD method at $S = 10$ for Regime 1 and Example 3

M	N	$T = 1$		$T = 10$	
		Price	Time (s)	Price	Time (s)
50	50	1.1779555	0.113	2.5193244	0.113
100	100	1.1756722	0.226	2.5458278	0.226
200	200	1.1750973	0.412	2.5534748	0.412
400	400	1.1749502	0.645	2.5553798	0.645
800	800	1.1749104	0.865	2.5558371	0.865
1600	1600	1.1748988	1.045	2.5559404	1.045
IOS [2]		1.174888119	5286	2.555962940	21570
LPI [2]		1.174888084	713	2.555963088	1015

Table 6 Maximum error and ratio for different number of spatial grids N and time steps M of RBF-FD method for American put option with two regimes for Example 3

M	N	$T = 1$				$T = 10$			
		Regime 1		Regime 2		Regime 1		Regime 2	
		Max error	Ratio	Max error	Ratio	Max error	Ratio	Max error	Ratio
50	50	4.7e−03		5.0e−03		3.8e−02		3.9e−02	
100	100	1.1e−03	2.006	1.2e−03	2.000	1.0e−02	1.834	1.0e−02	1.833
200	200	2.9e−04	2.022	3.0e−04	2.017	2.6e−03	2.049	2.6e−03	2.045
400	400	7.1e−05	2.037	7.5e−05	2.031	6.1e−04	2.100	6.1e−04	2.102
800	800	1.5e−05	2.159	1.7e−05	2.153	1.2e−04	2.266	1.2e−04	2.264

points are computed by RBF-FD method, and presented in Table 5. For comparison, option prices and CPU times of IOS and LPI methods reported in [2] are given at the button of Table 5. Results show that RBF-FD method is fast and accurate in comparison with IOS and LPI methods developed in [2]. Also, for different number of spatial grids and time steps, maximum error and ratio are derived for different values of maturity time and presented in Table 6.

Figure 3 displays the option values, Delta and Gamma functions, and also, in Fig. 4, we have plotted option price surfaces that are obtained with RBF-FD method for two different regimes and $T = 1$.

Example 4 Here, we report the numerical results when there are four regimes with the parameters

$$\begin{pmatrix} r_1 \\ r_2 \\ r_3 \\ r_4 \end{pmatrix} = \begin{pmatrix} 0.02 \\ 0.1 \\ 0.06 \\ 0.15 \end{pmatrix}, \quad \begin{pmatrix} \sigma_1 \\ \sigma_2 \\ \sigma_3 \\ \sigma_4 \end{pmatrix} = \begin{pmatrix} 0.9 \\ 0.5 \\ 0.7 \\ 0.2 \end{pmatrix}, \quad \mathbf{Q} = \begin{pmatrix} -1 & \frac{1}{3} & \frac{1}{3} & \frac{1}{3} \\ \frac{1}{3} & -1 & \frac{1}{3} & \frac{1}{3} \\ \frac{1}{3} & \frac{1}{3} & -1 & \frac{1}{3} \\ \frac{1}{3} & \frac{1}{3} & \frac{1}{3} & -1 \end{pmatrix}, \quad T = 1, \quad S_0 = 9.$$

Thus, the market can be in any of the four regimes with equal probability. In Table 7, we report the approximate prices of American put options in the four different regimes and different asset prices, obtained by using the RBF-FD approximation scheme, and since for

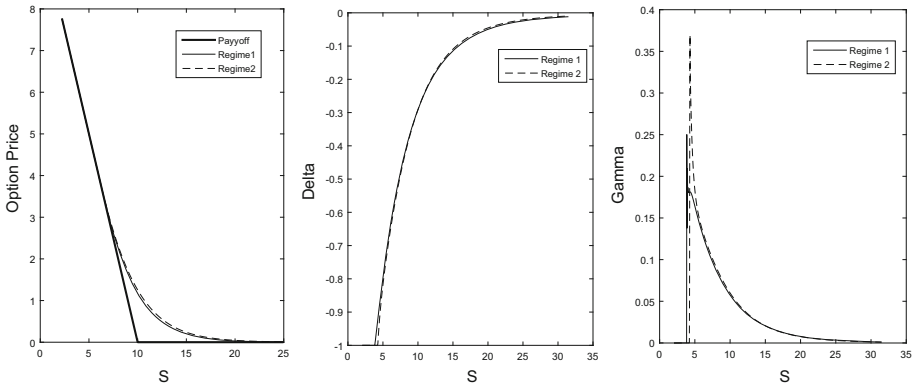

Fig. 3 Today's American put price, Delta and Gamma values for RBF-FD method and $T = 1$ with parameters as provided in Example 3

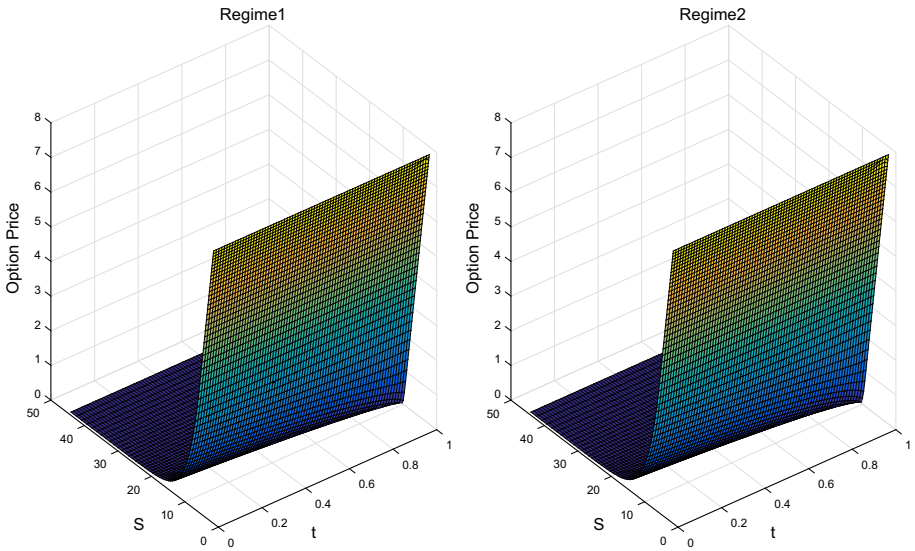

Fig. 4 The option price surface for two regimes derived by RBF-FD method and $T = 1$ with parameters as provided in Example 3

American cases there is no exact solution, so for comparison, we present numerical solutions obtained by FF-expl, ETD-CN and Tree methods given in literatures. The RBF-FD solutions are derived with $\triangle x = \triangle \tau = 0.01$, also condition number of arisen linear system is 30.475, and CPU time is 0.217 s.

For different number of spatial grids and time steps, results are derived by RBF-FD method including option *Price* at $S = S_0 = 9$, *Error*, *Ratio* and CPU *time(s)*, and presented in Table 8.

Figure 5 displays the option values, Delta and Gamma functions. Also, in Fig. 6, we have plotted option price surfaces that are obtained with RBF-FD method for four different regimes. Also, for different number of spatial grids and time steps, maximum error and ratio are computed for different regimes and reported in Table 9.

Table 7 American put option prices computed by RBF-FD with $\triangle x = \triangle \tau = 0.01$, FF-expl [16], ETD-CN [30] and Tree [33] methods at different asset prices for four regimes for Example 4

Regime	Method	$S = 7.5$	$S = 9$	$S = 10.5$	$S = 12$
1	RBF-FD	3.1424	2.5564	2.1052	1.7527
	FF-expl	3.1421	2.5563	2.1047	1.7524
	ETD-CN	3.1513	2.5641	2.1113	1.7578
	Tree	3.1433	2.5576	2.1064	1.7545
2	RBF-FD	2.2320	1.5835	1.1415	0.8377
	FF-expl	2.2313	1.5827	1.1406	0.8368
	ETD-CN	2.2384	1.5884	1.1451	0.8404
	Tree	2.2319	1.5834	1.1417	0.8377
3	RBF-FD	2.6744	2.0566	1.6013	1.2623
	FF-expl	2.6739	2.0559	1.6004	1.2614
	ETD-CN	2.6813	2.0623	1.6057	1.2658
	Tree	2.6746	2.0568	1.6014	1.2625
4	RBF-FD	1.6576	0.9857	0.6554	0.4708
	FF-expl	1.6573	0.9850	0.6546	0.4700
	ETD-CN	1.6664	0.9903	0.6580	0.4725
	Tree	1.6574	0.9855	0.6553	0.4708

Table 8 Numerical results derived by RBF-FD method with different number of spatial grids and time steps for American put option price at $S = 9$ with four regimes for Example 4

Regime	M	N	Price	Error	Ratio	Time (s)
1	50	50	2.5418456			0.024
	100	100	2.5531370	1.1e−02		0.092
	200	200	2.5561649	3.0e−03	1.899	0.138
	400	400	2.5569334	7.7e−04	1.978	0.513
	800	800	2.5571243	1.9e−04	2.009	2.092
2	50	50	1.5825090			0.024
	100	100	1.5832415	7.3e−04		0.092
	200	200	1.5834372	2.0e−04	1.904	0.138
	400	400	1.5834794	4.2e−05	2.213	0.513
	800	800	1.5834852	5.8e−06	2.857	2.092
3	50	50	2.0519000			0.024
	100	100	2.0555084	3.6e−03		0.092
	200	200	2.0564695	9.6e−04	1.909	0.138
	400	400	2.0567070	2.4e−04	2.017	0.513
	800	800	2.0567630	5.6e−05	2.085	2.092
4	50	50	0.9825651			0.024
	100	100	0.9848779	2.3e−03		0.092
	200	200	0.9855176	6.4e−04	1.854	0.138
	400	400	0.9856777	1.6e−04	1.999	0.513
	800	800	0.9857152	3.8e−05	2.093	2.092

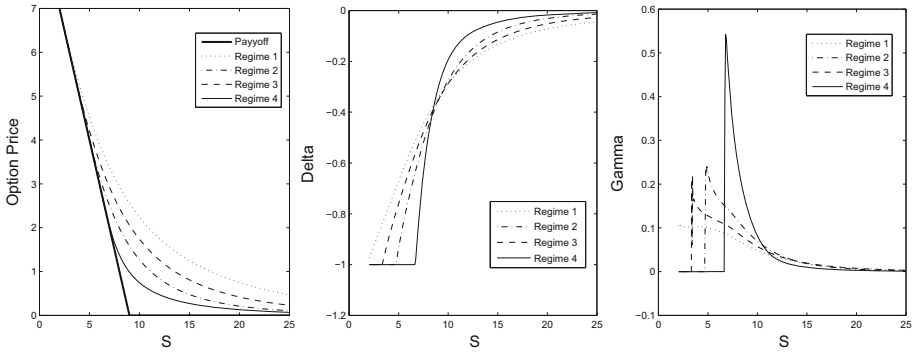

Fig. 5 Today's American put price, Delta and Gamma values for RBF-FD method with parameters as provided in Example 4

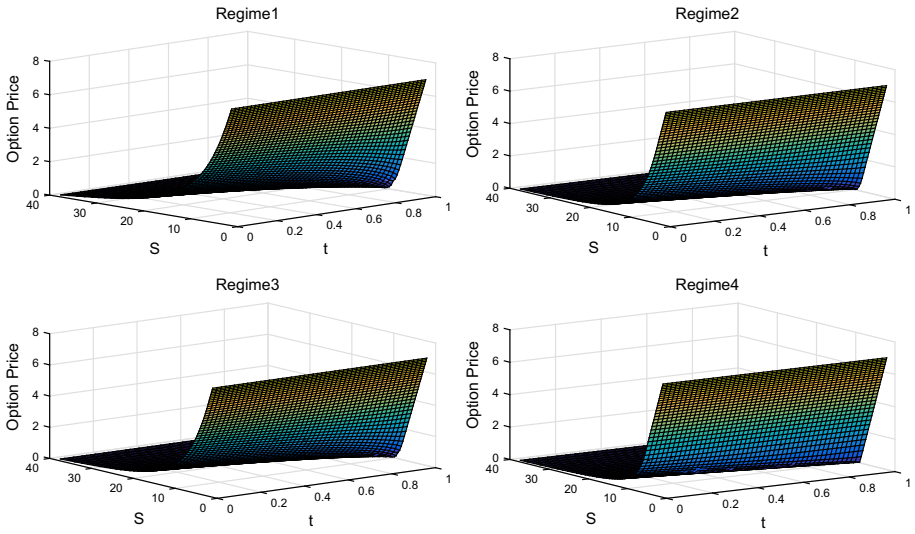

Fig. 6 The option price surface for four regimes derived by RBF-FD method with parameters as provided in Example 4

Table 9 Maximum error and ratio for different number of spatial grids N and time steps M of RBF-FD method for American put option with four regimes for Example 4

M	N	Regime 1		Regime 2		Regime 3		Regime 4	
		Max error	Ratio	Max error	Ratio	Max error	Ratio	Max error	Ratio
50	50	2.8e−02		4.8e−03		1.1e−02		7.7e−03	
100	100	7.7e−03	1.897	1.1e−03	2.052	3.0e−03	1.957	2.0e−03	1.951
200	200	1.9e−03	1.992	2.5e−04	2.174	7.3e−04	2.041	5.8e−04	1.782
400	400	4.6e−04	2.061	5.0e−05	2.341	1.6e−04	2.134	7.7e−05	2.911
800	800	9.6e−05	2.265	1.3e−05	1.944	3.1e−05	2.402	3.0e−05	1.353

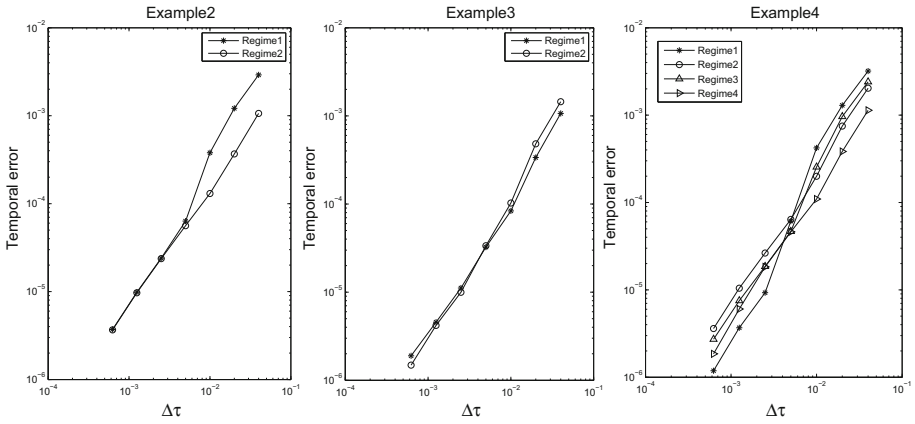

Fig. 7 Temporal error vs. $\triangle\tau$ derived by RBF-FD method with $N = 800$ spatial nodes and a sequence of seven increasing time steps $M = 25, 50, 100, 200, 400, 800, 1600$ for Examples 2, 3 and 4

To show convergence of the time discretisation, we numerically investigate the behavior of the global temporal errors as a function of $\triangle\tau$ which is defined by

$$\text{Temporal error} = \sqrt{\frac{1}{N}\sum_{j=1}^{N}\left(V_i^M(S_j,0) - V_i^{10\,000}(S_j,0)\right)^2}, \tag{54}$$

where V_i^M is the numerical solution of ith regime at the spatial nodes $S_j \in [\frac{S_0}{2}, \frac{3S_0}{2}]$, $j = 1, 2 \ldots, N$ where $N = 800$ after M time steps, and $V_i^{10\,000}$ is the corresponding solution for $M = 10{,}000$ and $N = 800$ used as an approximant for the exact solution. Figure 7 displays the global temporal errors versus $\triangle\tau$ for a sequence of seven increasing time steps M, namely 25, 50, 100, 200, 400, 800, 1600 and $N = 800$ for Examples 2, 3 and 4.

Example 5 For more comparison, in this example, we consider the following parameters

$$\begin{pmatrix} r_1 \\ r_2 \end{pmatrix} = \begin{pmatrix} 0.1 \\ 0.1 \end{pmatrix}, \quad \begin{pmatrix} \sigma_1 \\ \sigma_2 \end{pmatrix} = \begin{pmatrix} 0.4 \\ 0.2 \end{pmatrix}, \quad \mathbf{Q} = \begin{pmatrix} -1.375968919 & 1.375968919 \\ 1.031976689 & -1.031976689 \end{pmatrix},$$

$T = 1$ and $S_0 = 100$ adapted by [47] for pricing American put option under the regime switching model. In [47], finite element method combined with Crank–Nicolson scheme with 12800 time steps (CN12800) and the lattice method with 51200 time steps (LM51200) are considered, and we apply RBF-FD method with 800 time steps and 513 spatial grids (RBF-FD800), and results for American put option are reported in Table 10. Also, today's hedge ratios (Delta function values) for Crank–Nicolson scheme, lattice method and RBF-FD method for different asset prices are given in Table 11. Reported results in Tables 10 and 11 show that RBF-FD method provides not only very accurate values of option prices and hedge ratios, but also it is faster than Crank–Nicolson and lattice methods developed in [47].

The accuracy of global RBF methods highly depends on the shape parameter ε of the basis functions. For smooth problems, the best accuracy is typically achieved when ε is small, but then the condition number of the linear system becomes very large, but for local RBF methods such as RBF-FD the accuracy of the method is less sensitive to the changes of shape parameter. Figure 8 displays the dependence of the maximum error defined by (53)

Table 10 American put option values derived by Crank–Nicolson scheme with 12800 time steps (CN12800) and the lattice method with 51200 time steps (LM51200) in [47] and RBF-FD method with 800 time steps (RBF-FD800) for two regimes for Example 5

S	Regime 1			Regime 2		
	CN12800	LM51200	RBF-FD800	CN12800	LM51200	RBF-FD800
60	40.0000	40.0000	39.9999648	40.0000	40.0000	39.9999648
70	30.0007	30.0006	30.0007529	30.0000	30.0000	29.9999590
80	21.2289	21.2289	21.2289525	20.0000	20.0000	19.9999531
90	14.6191	14.6190	14.6191707	11.6126	11.6125	11.6125421
100	9.9245	9.9245	9.9246529	6.7423	6.7423	6.7423578
110	6.7017	6.7017	6.7018512	3.9244	3.9243	3.9244261
120	4.5257	4.5257	4.5258304	2.3083	2.3083	2.3084130
130	3.0665	3.0665	3.0667011	1.3825	1.3825	1.3826159
140	2.0889	2.0889	2.0890234	0.8460	0.8460	0.8460737
150	1.4318	1.4318	1.4319674	0.5287	0.5287	0.5287890

Table 11 Today's hedge ratios derived by Crank–Nicolson scheme with 12800 time steps (CN12800), the lattice method with 51200 time steps (LM51200) in [47] and RBF-FD method with 800 time steps (RBF-FD800) for two regimes for Example 5

S	Regime 1			Regime 2		
	CN12800	LM51200	RBF-FD800	CN12800	LM51200	RBF-FD800
60	−1.0000	−1.0000	−1.0000311	−1.0000	−1.0000	−1.0000311
70	−0.9942	−0.9941	−0.9939012	−1.0000	−1.0000	−1.0000311
80	−0.7667	−0.7667	−0.7667411	−1.0000	−1.0000	−1.0000308
90	−0.5586	−0.5586	−0.5586468	−0.6319	−0.6319	−0.6318931
100	−0.3881	−0.3881	−0.3881526	−0.3664	−0.3664	−0.3664050
110	−0.2636	−0.2636	−0.2636018	−0.2109	−0.2109	−0.2109330
120	−0.1771	−0.1771	−0.1771089	−0.1206	−0.1206	−0.1206398
130	−0.1186	−0.1186	−0.1186200	−0.0694	−0.0694	−0.0694222
140	−0.0796	−0.0796	−0.0795718	−0.0406	−0.0406	−0.0406406
150	−0.0536	−0.0536	−0.0536103	−0.0243	−0.0243	−0.0243355

on the size of the shape parameter. For computing maximum errors, we use $N = 2400$ and $M = 2400$ and $\varepsilon = 0.5$ for reference solution $\widetilde{U}_i^{ref}(x, T)$ and also, we let $N = 400$ and $M = 400$ and derive RBF-FD solution $\widetilde{U}_i(x, T)$ for different values of shape parameter.

8 Conclusion

We proposed RBF-FD method to price European and American options under the regime switching model. The free boundary problem formulated as a PDE was transformed into an LCP problem. The RBF-FD was used for the spatial discretisation. Next, a Crank–Nicolson time discretisation was combined with an operator splitting method. This results in a linear algebraic system with a sparse and well-conditioned matrix. Also, we proved the resulting

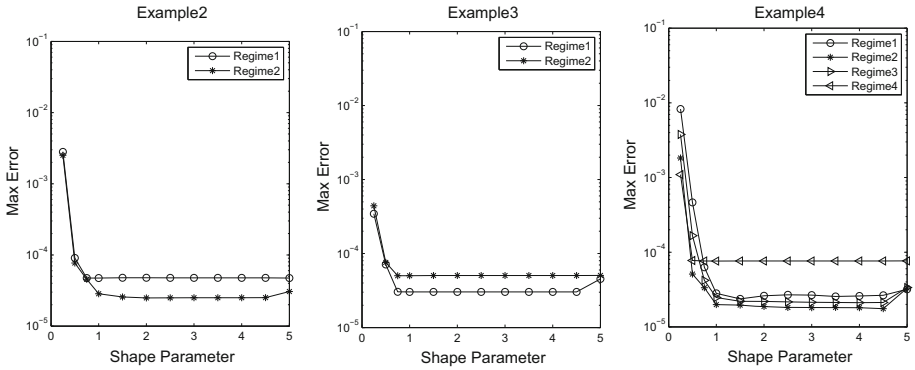

Fig. 8 Maximum error against the shape parameter ε

linear system of equations after space and time discretization is uniquely solvable and stable. The shape parameter in the RBF method affects the accuracy and stability of the method, but the proposed local RBF method is less sensitive to the change of the shape parameter. The effect of the time discretisation is measured by studying the temporal error for American option cases. The numerical experiments confirm that RBF-FD performs not only better than the front-fixing explicit method, the exponential time differencing Crank–Nicolson scheme, the binomial tree approach and finite element method but also, it is faster than iterated optimal stopping and local policy iteration methods.

Acknowledgements H. Li was supported in part by the NSF Grant DMS-1819041, and by the Wayne State University Career Development Chair Award.

References

1. Andersen, L.: Markov models for commodity futures: theory and practice. Quant. Finance **10**(8), 831–854 (2010)
2. Babbin, J., Forsyth, P.A., Labahn, G.: A comparison of iterated optimal stopping and local policy iteration for American options under regime switching. J. Sci. Comput. **58**(2), 409–430 (2014)
3. Ballestra, L.V., Pacelli, G.: Pricing European and American options with two stochastic factors: a highly efficient radial basis function approach. J. Econ. Dyn. Control **37**(6), 1142–1167 (2013)
4. Bansal, R., Zhou, H.: Term structure of interest rates with regime shifts. J. Finance **57**(5), 1997–2043 (2002)
5. Bastani, A.F., Ahmadi, Z., Damircheli, D.: A radial basis collocation method for pricing American options under regime-switching jump-diffusion models. Appl. Numer. Math. **65**, 79–90 (2013)
6. Bayona, V., Moscoso, M., Carretero, M., Kindelan, M.: RBF-FD formulas and convergence properties. J. Comput. Phys. **229**(22), 8281–8295 (2010)
7. Berman, A., Plemmons, R.J.: Nonnegative Matrices in the Mathematical Sciences. Academic Press, New York (1994)
8. Black, F., Scholes, M.: The pricing of options and corporate liabilities. J. Polit. Econ. **81**(3), 637–654 (1973)
9. Borici, A., Lüthi, H.-J.: Pricing American put options by fast solutions of the linear complementarity problem. In: Kontoghiorghes, E.J., Rustem, B., Siokos, S. (eds.) Computational Methods in Decision-Making, Economics and Finance, pp. 325–338. Springer, New York (2002)
10. Boyle, P., Draviam, T.: Pricing exotic options under regime switching. Insur. Math. Econ. **40**(2), 267–282 (2007)
11. Buffington, J., Elliott, R.J.: American options with regime switching. Int. J. Theor. Appl. Finance **05**(05), 497–514 (2002)

12. Chen, S., Insley, M.: Regime switching in stochastic models of commodity prices: an application to an optimal tree harvesting problem. J. Econ. Dyn. Control **36**(2), 201–219 (2012)
13. Chen, Z., Forsyth, P.A.: Implications of a regime-switching model on natural gas storage valuation and optimal operation. Quant. Finance **10**(2), 159–176 (2010)
14. Dai, M., Zhang, Q., Zhu, Q.J.: Trend following trading under a regime switching model. SIAM J. Financ. Math. **1**(1), 780–810 (2010)
15. Driscoll, T.A., Hale, N., Trefethen, L.N.: Chebfun Guide. Pafnuty Publications, Oxford (2014)
16. Egorova, V.N., Company, R., Jódar, L.: A new efficient numerical method for solving American option under regime switching model. Comput. Math. Appl. **71**(1), 224–237 (2016)
17. Fasshauer, G.E., Khaliq, A.Q.M., Voss, D.A.: Using meshfree approximation for multiasset American options. J. Chin. Inst. Eng. **27**(4), 563–571 (2004)
18. Fornberg, B., Flyer, N.: A Primer on Radial Basis Functions with Applications to the Geosciences. SIAM, Philadelphia (2015)
19. Fornberg, B., Flyer, N.: Solving PDEs with radial basis functions. Acta Numer. **24**, 215–258 (2015)
20. Golbabai, A., Mohebianfar, E.: A new method for evaluating options based on multiquadric RBF-FD method. Appl. Math. Comput. **308**(Supplement C), 130–141 (2017)
21. Guo, X.: Information and option pricings. Quant. Finance **1**(1), 38–44 (2001)
22. Haldrup, N., Nielsen, M.O.: A regime switching long memory model for electricity prices. J. Econ. **135**(12), 349–376 (2006)
23. Hardy, M.: A regime-switching model of long-term stock returns. N. Am. Actuar. J. **5**(2), 41–53 (2001)
24. Holmes, A.D., Yang, H., Zhang, S.: A front-fixing finite element method for the valuation of American options with regime switching. Int. J. Comput. Math. **89**(9), 1094–1111 (2012)
25. Hon, Y.C., Mao, X.Z.: A radial basis function method for solving options pricing model. Financ. Eng. **8**, 31–49 (1999)
26. Huang, Y., Forsyth, P.A., Labahn, G.: Methods for pricing American options under regime switching. SIAM J. Sci. Comput. **33**(5), 2144–2168 (2011)
27. Howison, S., Wilmott, P., Dewynne, J.: Option Pricing: Mathematical Models and Computation. Oxford Financial Press, Oxford (1993)
28. Ikonen, S., Toivanen, J.: Operator splitting methods for American option pricing. Appl. Math. Lett. **17**(7), 809–814 (2004)
29. Kanas, A.: On real interest rate dynamics and regime switching. J. Bank. Finance **32**(10), 2089–2098 (2008)
30. Khaliq, A.Q.M., Kleefeld, B., Liu, R.H.: Solving complex PDE systems for pricing American options with regime-switching by efficient exponential time differencing schemes. Numer. Methods Partial Differ. Equ. **29**(1), 320–336 (2013)
31. Khaliq, A.Q.M., Liu, R.H.: New numerical scheme for pricing American option with regime-switching. Int. J. Theor. Appl. Finance **12**(03), 319–340 (2009)
32. Le, H., Wang, C.: A finite time horizon optimal stopping problem with regime switching. SIAM J. Control Optim. **48**(8), 5193–5213 (2010)
33. Liu, R.H.: Regime-switching recombining tree for option pricing. Int. J. Theor. Appl. Finance **13**(03), 479–499 (2010)
34. Liu, R.H., Nguyen, D.: A tree approach to options pricing under regime-switching jump diffusion models. Int. J. Comput. Math. **92**(12), 2575–2595 (2015)
35. Mollapourasl, R., Fereshtian, A., Vanmaele, M.: Radial basis functions with partition of unity method for American options with stochastic volatility. Comput. Econ. (2017). https://doi.org/10.1007/s10614-017-9739-8
36. Pettersson, U., Larsson, E., Marcusson, G., Persson, J.: Improved radial basis function methods for multi-dimensional option pricing. J. Comput. Appl. Math. **222**(1), 82–93 (2008). **(Special issue: numerical PDE methods in finance)**
37. Pooley, D.M., Vetzal, K.R., Forsyth, P.A.: Convergence remedies for non-smooth payoffs in option pricing. J. Comput. Finance **6**(4), 25–40 (2003)
38. Rad, J.A., Parand, K., Ballestra, L.V.: Pricing European and American options by radial basis point interpolation. Appl. Math. Comput. **251**(Supplement C), 363–377 (2015)
39. Safdari-Vaighani, A., Heryudono, A., Larsson, E.: A radial basis function partition of unity collocation method for convection–diffusion equations arising in financial applications. J. Sci. Comput. **64**(2), 341–367 (2015)
40. Salmi, S., Toivanen, J.: An iterative method for pricing American options under jump-diffusion models. Appl. Numer. Math. **61**(7), 821–831 (2011)
41. Seydel, R.: Tools for Computational Finance, 4th edn. Springer, Berlin (2009)

42. Shcherbakov, V., Larsson, E.: Radial basis function partition of unity methods for pricing vanilla basket options. Comput. Math. Appl. **71**(1), 185–200 (2016)
43. Varga, R.S.: Matrix Iterative Analysis. Springer, Berlin (2010)
44. Wahab, M.I.M., Yin, Z., Edirisinghe, N.C.P.: Pricing swing options in the electricity markets under regime-switching uncertainty. Quant. Finance **10**(9), 975–994 (2010)
45. Wendland, H.: Scattered Data Approximation. Number 17 in Cambridge Monographs on Applied and Computational Mathematics. Cambridge University Press, New York (2005)
46. Wu, Z., Hon, Y.C.: Convergence error estimate in solving free boundary diffusion problem by radial basis functions method. Eng. Anal. Bound. Elem. **27**(1), 73–79 (2003)
47. Yang, H.: A numerical analysis of American options with regime switching. J. Sci. Comput. **44**(1), 69–91 (2010)
48. Yin, G., Zhang, Q.: Continuous-Time Markov Chains and Applications: A Singular Perturbation Approach. Springer, Berlin (1998)
49. Young, D.M.: Iterative Solution of Large Linear Systems. Academic Press, New York (1971)
50. Yousuf, M., Khaliq, A.Q.M., Liu, R.H.: Pricing American options under multi-state regime switching with an efficient L-stable method. Int. J. Comput. Math. **92**(12), 2530–2550 (2015)
51. Zhang, Q., Zhou, X.Y.: Valuation of stock loans with regime switching. SIAM J. Control Optim. **48**(3), 1229–1250 (2009)
52. Zvan, R., Forsyth, P.A., Vetzal, K.R.: Penalty methods for American options with stochastic volatility. J. Comput. Appl. Math. **91**(2), 199–218 (1998)